Transactions of the Materials Research Society of Japan 33[2] 291-294 (2008)

Toward the Realization of Half-Metallic Antiferromagnetism for Future Spintronics

Masao Nakao
Department of Precision Engineering, Tokai University, 1117 Kitakaname, Hiratsuka, Kanagawa 259-1292, Japan
Fax: 81-463-58-1211, e-mail: mnakao@keyaki.cc.u-tokai.ac.jp

We present results based on first-principles calculations of a computational search for half-metallic (HM) ferromagnetic (FM) and antiferromagnetic (AFM) materials within the class of zinc-blende-structure pnictides and chalcogenides that incorporate 3*d*-transition-metal ions. Six HM-FM results are found for pnictides (VAs, VSb, CrAs, CrSb, MnAs, and MnSb) and four results for chalcogenides (VSe, VTe, CrSe, and CrTe). Theoretically predicted HM-AFM's with no net magnetization, or fully compensated ferrimagnetic materials, represent a fundamentally different state of matter. A promising possibility is in ternary systems such as chalcopyrites and [001]-oriented monolayer superlattices containing either transition-metal pair: CrFe or VCo. This study provides viable candidates for these unusual magnetic materials that would be realized using atomic-layer-by-layer growth techniques for future spintronic applications.
Key words: half-metal, antiferromagnet, magnetic superlattice, electronic band structure

1. INTRODUCTION

For future spin electronics or *spintronics*, where it is not only the electron charge but also the electron spin that carries information, it is essential to inject spins from highly spin-polarized ferromagnets into nonmagnetic semiconductors. So far, spin-polarized hole injection from diluted magnetic semiconductors (DMS's) to III-V and II-VI semiconductors has already been demonstrated [1,2]. In the most promising Mn-doped GaAs, however, the Curie temperature T_C is as low as 110 K due to the limited solubility of Mn in GaAs [3].

Half-metals (HM's) have received considerable interest in recent years because of the complete polarization of carriers [4]. These materials can be regarded as a fundamentally different magnetic state of matter, in which the electrons responsible for the metallic behavior share the same spin while the electrons with the opposite spin are insulating. The Pauli spin susceptibility vanishes because of the absence of low energy spin-flip transitions available to the system. As a result of having a band gap at the Fermi energy (E_F) for one spin channel, the spin magnetic moment is an integer value in a stoichiometric HM. After de Groot *et al.* [5] initially predicted the half-metallic behavior of $C1_b$-type Heusler alloys, NiMnSb and PtMnSb, such a behavior was found in various perovskite structures [6,7] and rutile-structured CrO_2 [7,8]. Although these oxides were proved practically 100% spin polarized, besides their low T_C the stoichiometry of oxides is difficult to control and defects limit coherent carrier transport.

Another class of prospective HM's is zinc-blende (ZB) transition-metal pnictides and chalcogenides [9], which are compatible with ordinary III-V and II-VI semiconductors. As these compounds can be viewed as the 100% doping limit of DMS's, they are generally metastable in the ZB structure. In the bulk, they crystallize in either the hexagonal NiAs or the orthorhombic MnP structure as the ground state. The stable NiAs phase is a metallic ferromagnet or an antiferromagnet but show no gap. Recent molecular-beam-epitaxy (MBE) techniques, however, enable us to grow the ZB phase of CrAs [10], MnAs [11], and CrSb [12].

In addition to ferromagnetic (FM) parallel spin arrangements, ferrimagnetic or antiferromagnetic (AFM) alignments are also possible in ternary or more complicated systems. In particular, *half-metallic antiferromagnets* (HM-AFM's) [13] possess no macroscopic magnetization, yet their carriers are fully spin polarized. Besides conceivable applications as an ideal tip in a spin-polarized STM and a stable spin-polarized electrode in a junction device, HM-AFM's provide a possibility of "single spin superconductivity" [14] due to triplet (spin-parallel) Cooper pairs in the metallic channel. Since the initial theoretical prediction of a Heusler-based HM-AFM [13,15], several candidates have been reported in double perovskites [16] and thiospinels [17]. Despite several experimental challenges, no actual HM-AFM's have been synthesized yet.

We report here results of a computational search for HM-FM and HM-AFM members within the class of binary and ternary ZB-derived 3*d*-transition-metal compounds with tetrahedral coordination by means of a first-principles density functional method. In contrast with octahedrally coordinated HM's such as the metallic Heusler alloys and the ionic double perovskites, relatively large exchange splitting and, therefore, a wide HM gap in the covalent tetrahedral structure can be expected. The origin of this behavior is the *p–d* hybridization due to the symmetry of crystal fields.

2. FIRST-PRINCIPLES RESULTS

2.1 Computational method

Self-consistent band-structure calculations are based on the WIEN2k package [18] for the scalar relativistic hybrid full-potential augmented plane-wave plus local-orbitals method within the framework of spin-polarized density-functional theory (DFT). We employ the semirelativistic approximation and the core

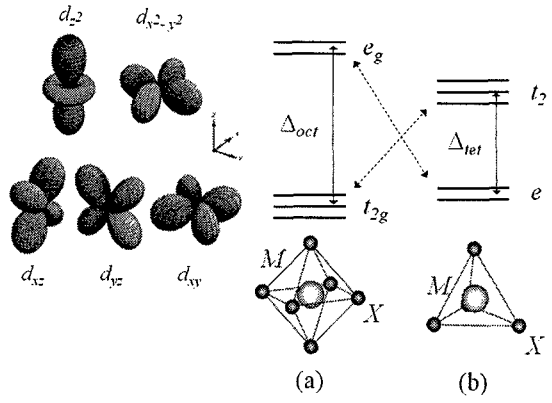

Fig. 1. Crystal-field-splitting diagrams representing the d states of binary transition-metal compounds MX with both (a) octahedral and (b) tetrahedral coordination.

levels are treated fully relativistically. Spin-orbit coupling is included in a second-variational procedure using the scalar-relativistic wavefunctions as basis. The electrons exchange-correlation potential is described with the generalized gradient approximation (GGA) using the Perdew-Berke-Ernzerhof functional parameterization. The plane-wave cutoff is determined by $R_{MT}K_{max}$ = 8.0 (where R_{MT} is the muffin-tin radius, and K_{max} is the maximum modulus for the reciprocal lattice vector). The Brillouin zone is sampled on a uniform mesh with 5000 k points for ZB binary systems and 2000 k points for ternary systems in the entire Brillouin zone. The muffin-tin radii R_{MT} are chosen as touching spheres to keep as much core charge inside the muffin-tin sphere as possible.

2.2 Half-metallic ferromagnets

In order to quantify the effect of crystal fields, we compare the d states of binary transition-metal compounds MX with both octahedral and tetrahedral coordination, as shown schematically in Fig. 1. The crystal field splits the degeneracy of five d states of the transition-metal (cation) M into doubly degenerated d e_g states and triply degenerated d t_{2g} states. In an octahedral crystal field, the d e_g state will be higher in energy than the d t_{2g} state. The splitting observed in a tetrahedral field, however, is the opposite of the octahedral case. (The subscript g is omitted for lack of inversion symmetry in this geometry.) Since a linear combination of the p states of the four neighboring nonmetallic atoms (anions) X have the same t_2 symmetry and large overlapping of orbitals, the M d t_2 states hybridize strongly with the X p states. This symmetry-induced p–d hybridization forms a lower p–d t_2 bonding state (BS) with X 4p character and a higher p–d t_2 antibonding state (ABS) with M 3d character, suggesting the occurrence of electron transfer from filled X p states to vacant M d t_2 states. Thus, strong exchange correlation between M cations via the common X anions is expected [19,20]. In contrast, the d e state is nonbonding in nature. Octahedral compounds generally show strong *ionicity* in (closed-shell) insulators or *metallicity* in (open-shell) conductors while tetrahedral compounds are typically covalent.

Half-metallicity can be readily distinguished by the spin-resolved total densities of states (DOS's) for possible 3d-transition-metal pnictides (shown in Fig. 2) and chalcogenides (in Fig.3) whose lattice parameters are optimized. The calculated equilibrium lattice parameters are listed in Tables I and II, respectively. Among the candidates, we find six results for pnictides (VAs, VSb,

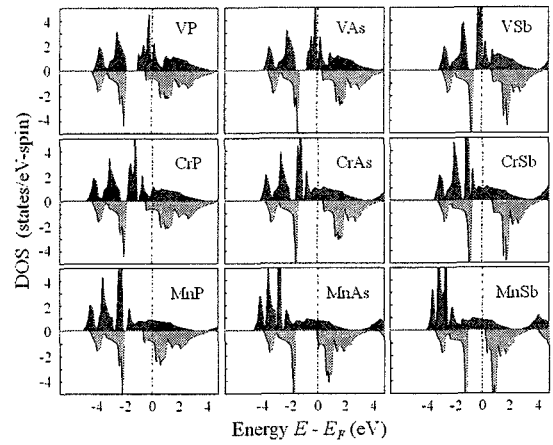

Fig. 2 Spin-resolved total densities of states (DOS's) for possible 3d-transition-metal pnictides whose lattice parameters are optimized. Six compounds (VAs, VSb, CrAs, CrSb, MnAs, and MnSb) are bulk HM's.

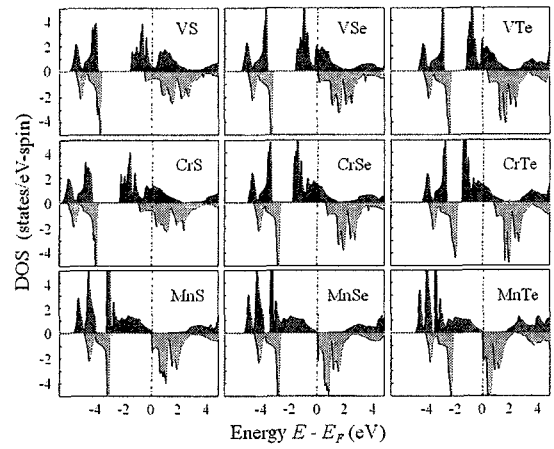

Fig. 3 Spin-resolved total densities of states (DOS's) for possible 3d-transition-metal chalcogenides whose lattice parameters are optimized. Four compounds (VSe, VTe, CrSe, and CrTe) are bulk HM's.

Table I. Calculated equilibrium lattice parameters (a) of the 3d-transition-metal pnictides.

MX	a (Å)	MX	a (Å)	MX	a (Å)
VP	5.47	VAs	5.72	VSb	6.20
CrP	5.33	CrAs	5.68	CrSb	6.15
MnP	5.33	MnAs	5.73	MnSb	6.23

Table II. Calculated equilibrium lattice parameters (a) of the 3d-transition-metal chalcogenides.

MX	a (Å)	MX	a (Å)	MX	a (Å)
VS	5.39	VSe	5.82	VTe	6.26
CrS	5.20	CrSe	5.85	CrTe	6.29
MnS	5.62	MnSe	5.95	MnTe	6.40

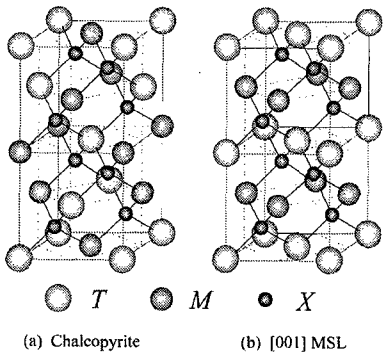

Fig. 4. Crystal structures of (a) the chalcopyrite TMX_2 and (b) the [001]-oriented monolayer superlattice (MSL) TX/MX.

CrAs, CrSb, MnAs, and MnSb) and four results for chalcogenides (VSe, VTe, CrSe, and CrTe) to be characteristic of HM's. In Fig. 2, the Fermi energies E_F of phosphide systems cut across the conduction band in the spin-down channel, so that spin-down electrons also contribute to conductivity. Fe and heavier systems prefer AFM arrangements. In Fig. 3, the DOS behaviors of sulfide systems are quite similar to the phosphide systems. Moreover, Mn and heavier systems favor AFM couplings.

2.3 Half-metallic antiferromagnets

The simplest way to achieve the requirements of the net moment to be exactly zero is to have a unit cell with two distinct magnetic ions whose moments are equal in magnitude but antialigned. Tetrahedral ternary systems have a few polytypes formed by different stacking of basic atomic planes. The chalcopyrite structure TMX_2 shown in Fig. 4(a) is derived from the cubic ZB structure; the presence of two different cations (T and M) ordered at the half tetrahedral sites yields a doubling of the ZB unit cell along the c direction. The anion (X) in the other face-centered cubic sublattice has four first nearest neighbors: two T and two M atoms. As a consequence, the chalcopyrite has tetragonal symmetry with space group $I\bar{4}2d$. Thus, the d e state splits into e_a (= d_{z^2}) and e_b (= $d_{x^2-y^2}$) states, whereas the d t_2 state splits into a doubly degenerated t_a (= $d_{xz} + d_{yz}$) state and a single t_b (= d_{xy}) state. In addition to the cell dimensions a and c, for which we define the tetragonal ratio $\eta = c/2a$ the structure is characterized by the anion displacement parameter u in units of a. When $\eta = 1$ ($2a = c$) and $u = 0.25$, the atoms are on the sites of the ZB structure.

Figure 5 presents the trend in DOS's characteristic of two series of chalcopyrites $CrFeX_2$ and $VCoX_2$ (X = S, Se, and Te) whose lattice parameters are optimized [20]. The equilibrium lattice parameters and the total energy difference between the AFM and FM states, which is a measure of magnetic coupling between Cr (V) and Fe (Co) spins, are listed in Table III. The GGA calculations indeed lead to HM-AFM solutions at the equilibrium lattice parameters. The AFM ground state is low enough in energy (compared with the FM state) to show the HM-AFM character at room temperature. The paramagnetic state is even higher than the FM state. Their overall behaviors in the series are quite similar. Briefly, the symmetry-induced p–d hybridization takes place between every cations and anions. The HM gap in the spin-down channel can be explained in terms of the exchange splitting, being proportional to the local magnetic moments in a unit cell. Their electronic configurations of 3d magnetic ions are nominally d^4–d^6 and d^3–d^7, respectively. Electron transfer via the common anions determines the magnetic coupling between both cations and thus the magnitudes of local moments. For heavier anions, the HM gap becomes wider.

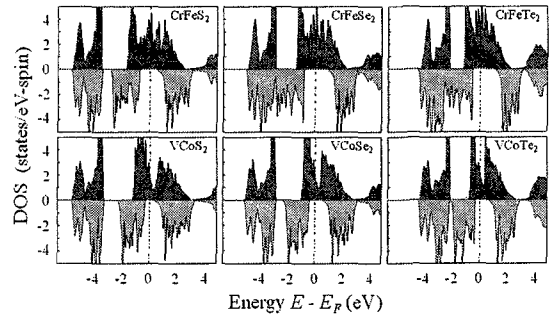

Fig. 5 Trend in DOS's characteristic of two series of chalcopyrites $CrFeX_2$ and $VCoX_2$ (X = S, Se, and Te) whose lattice parameters are optimized.

Table III. Calculated equilibrium lattice parameters (a, c, η, and u) and the total energy differences between the half-metallic antiferromagnetic (HM-AFM) and ferromagnetic (FM) states ($\Delta E = E_{HM\text{-}AFM} - E_{FM}$ in eV per formula unit) of the chalcopyrites TMX_2..

TMX_2	a (Å)	c (Å)	η	u	ΔE
$CrFeS_2$	5.31	10.76	1.012	0.255	-0.73
$CrFeSe_2$	5.69	11.55	1.015	0.256	-0.60
$CrFeTe_2$	6.13	12.47	1.018	0.257	-0.38
$VCoS_2$	5.24	10.56	1.007	0.262	-0.37
$VCoSe_2$	5.53	11.36	1.027	0.261	-0.35
$VCoTe_2$	6.10	12.03	0.987	0.263	-0.25

The crystal structures of chalcopyrites can be thought of as $(TX)_2(MX)_2$ superlattices in the [201] orientation. Artificial synthesis requires simpler structures. A monolayer superlattice (MSL; i.e., a CuAu-like pseudobinary compound) shown in Fig. 4(b) has the simple tetragonal structure with space group $P\bar{4}m2$. The length of a and b axes corresponds to a half of the face diagonal of the cubic cell. In addition to the cell dimensions a and c, for which we define the tetragonal ratio $\eta = c/(\sqrt{2}a)$, the structure is characterized by the anion displacement parameter u which measures, in units of c, the interplanar spacing between the T and X (001) planes along the c axis. When $\eta = 1$ and $u = 0.25$, the atoms are on the sites of the ZB structure. A [110]-oriented MSL is equivalent to a [001] MSL in the crystal structure.

Again, the trend in DOS's for two series of MSL's CX/FeX and VX/CoX (X = S, Se, and Te) is shown in Fig. 6. Basically it is quite similar to the chalcopyrite case. The optimized lattice parameters and the total energy differences between the HM-AFM and FM states are listed in Table IV. This similarity strongly suggests that the exchange correlations between magnetic ions depend merely on their local atomic environments and little on long-range atomic ordering. Like the chalcopyrite, indeed, this type of MSL's contains only T_2M_2 tet-

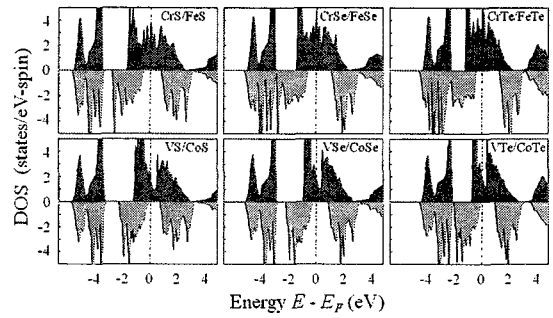

Fig. 6 Trend in DOS's characteristic of two series of [001]-oriented MSL's Cr*X*/Fe*X* and V*X*/Co*X* (*X* = S, Se, and Te) whose lattice parameters are optimized.

Table IV. Calculated equilibrium lattice parameters (*a*, *c*, η, and *u*) and the total energy differences between the half-metallic antiferromagnetic (HM-AFM) and ferromagnetic (FM) states ($\Delta E = E_{\text{HM-AFM}} - E_{\text{FM}}$ in eV per formula unit) of the [001]-oriented MSL's *TX*/*MX*.

TX/*MX*	*a*	*c*	η	*u*	ΔE
CrS/FeS	3.80	5.24	0.975	0.256	-0.72
CrSe/FeSe	4.04	5.57	0.993	0.257	-0.60
CrTe/FeTe	4.34	6.19	1.010	0.257	-0.38
VS/CoS	3.71	5.31	1.013	0.261	-0.36
VSe/CoSe	3.97	5.57	0.994	0.261	-0.37
VTe/CoTe	4.27	6.06	1.004	0.263	-0.27

rahedral clusters around the common *X* anion.

To understand the HM-AFM electronic structure in more detail, we consider the schematic model, dubbed the *ghost-bond-orbital model* (GBOM) [19,20], of the [001]-oriented MSL *TX*/*MX* pictured in Fig. 7. The open circles represent transition-metal cations *T* and *M* with *d* t_2 and *d e* orbitals; then, the neighboring black circles are nonmetallic anions *X*. The black and open dots within the ovals represent electrons and holes in the bond orbitals, respectively. The *d* t_2 states hybridize strongly with

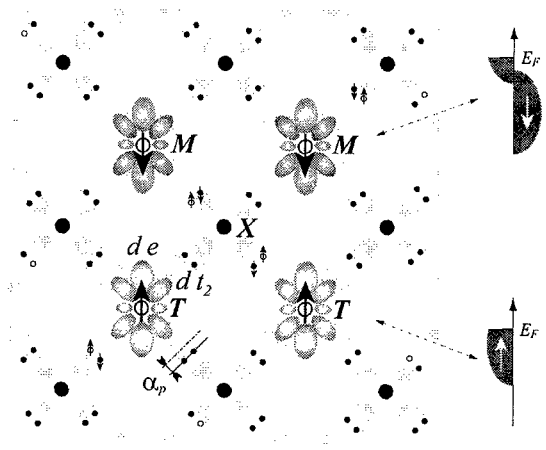

Fig. 7. Schematic *ghost-bond-orbital model* (GBOM) of the [001]-oriented MSL *TX*/*MX* viewed in the [100] direction. The open circles represent transition-metal cations (*T* and *M*) with *d* t_2 and *d e* orbitals; the neighboring black circles are anions (*X*). The black and open dots within the ovals represent electrons and holes in the bond orbitals, respectively.

the *p* states of the four neighboring anions, whereas the *d e* state is nonbonding in nature. The *p*–*d* hybridization effect removes electrons from the bond orbitals, and adds them to the *d* states. Holes produced in this process will mediate the magnetic coupling between cations through the common anions.

3. SUMMARY

This computational search indicates that the tetrahedral class of 3*d*-transition-metal compounds provides a fertile ground for HM's. The total-energy GGA calculations demonstrate that six pnictides (VAs, VSb, CrAs, CrSb, MnAs, and MnSb) and four chalcogenides (VSe, VTe, CrSe, and CrTe) are bulk HM's. Furthermore, the chalcopyrites (Cr$Fe X_2$ and V$Co X_2$) and [001]-oriented MSL's (Cr*X*/FeX and V*X*/Co*X*) are indeed bulk HM-AFM's, which possess no spontaneous magnetization, yet their conduction electrons are fully spin polarized. Their HM characteristics would be stable even at room temperature. Since the bonding nature is typically covalent in tetrahedral systems, the employment of GBOM is effective for the description of the HM-AFM electronic structures. Although all of these tetrahedral compounds are structurally metastable, with the development of recent synthesis techniques such as MBE and metalorganic chemical vapor deposition (MOCVD), atomic layer-by-layer growth would make it possible to realize a variety of predicted tetrahedral HM's for future spintronic applications.

References

[1] Y. Ohno, D. K. Young, B. Beschoten, F. Matsukura, H. Ohno, and D. Awschalom, *Nature* (London), **402**, 790 (1999).
[2] R. Fiederling, M. Keim, G. Reuscher, W. Ossau, G. Schmidt, A. Waag, and L. W. Molenkamp, *Nature* (London), **402**, 787 (1999).
[3] H. Ohno, *J. Magn. Magn. Mater.*, **200**, 110 (1999).
[4] W. E. Pickett and J. S. Moodera, *Phys. Today*, **54**, 39 (2001).
[5] R. A. de Groot, F. M. Mueller, P. G. van Engen, and K. H. J. Buschow, *Phys. Rev. Lett.*, **50**, 2024 (1983).
[6] J.-H. Park, E. Vescovo, C. K. H.-J. Kim, R. Ramesh, and T. Venkatesan, *Nature* (London), **392**, 794 (1998).
[7] R. J. Soulen, Jr. *et al.*, *Science*, **282**, 85 (1998).
[8] K. Schwarz, *J. Phys. F: Met. Phys.*, **16**, L211 (1986).
[9] P. Mavropoulos and I. Galanakis, *J. Phys.: Condens. Matter*, **19**, 315221 (2007).
[10] H. Akinaga, T. Manago, and M. Shirai, *Jpn. J. Appl. Phys.*, Part 2, **39**, L1118 (2000).
[11] K. Ono, J. Okabayashi, M. Mizuguchi, M. Oshima, A. Fujimori, and H. Akinaga, *J. Appl. Phys.*, **91**, 8088 (2002).
[12] J. H. Zhao, F. Matsukura, T. Takamura, D. C. E. Abe, and H. Ohno, *Appl. Phys. Lett.*, **79**, 2776 (2001).
[13] H. van Leuken and R. A. de Groot, *Phys. Rev. Lett.*, **74**, 1171 (1995).
[14] W. E. Pickett, *Phys. Rev. Lett.*, **77**, 3185 (1996).
[15] S. Wurmehl, H. C. Kandpal, G. H. Fecher, and C. Felser, *J. Phys.: Condens. Matter*, **18**, 6171 (2006).
[16] W. E. Pickett, *Phys. Rev.*, B **57**, 10613 (1998).
[17] M. S. Park, S. K. Kwon and B. I. Min, *Phys. Rev.*, B **64**, 100403 (2001).
[18] P. Blaha, K. Schwarz, G. K. H. Madsen, D. Kvasnicka, and J. Luitz, WIEN2k, An APW+*lo* Program for Calculating Crystal Properties (Techn. University Wien, Austria, 2001).
[19] M. Nakao, *Phys. Rev.*, B **69**, 214429 (2004).
[20] M. Nakao, *Phys. Rev.*, B **74**, 172404 (2006).

(Recieved September 7, 2007 ; Accepted December 13, 2007)